PERGAMON

Chemical Engineering Science 56 (2001) 771–778

Chemical Engineering Science

www.elsevier.nl/locate/ces

# Spatiotemporal patterns in models of cross-flow reactors. Regular and oscillatory kinetics

Olga Nekhamkina, Boris Y. Rubinstein, Moshe Sheintuch*

*Department of Chemical Engineering, Technion - I.I.T., Technion City, Haifa 32 000, Israel*

**Abstract**

We simulate and analyze the behavior of stationary and moving spatially periodic patterns in a simple cross-flow reactor with a first-order exothermic reactor and realistically high *Pe* and *Le*. Novel nonTuring stationary patterns emerge due to reactor–diffusion–convection interaction in the simple model that incorporates only concentration and temperature as its variables. We extend our previous analysis to account for reversible changes in a catalytic activity. We conduct linear and weakly nonlinear analysis around the critical point — the perturbation amplification threshold, as well as numerical simulations. For the limit case $Pe \to \infty$ the spatial behavior of the distributed system is analogous to the temporal behavior of the related CSTR problem. In the vicinity of the bifurcation point the emerging spatiotemporal patterns drastically depends on the type of a phase plane and both regular and aperiodic (chaotic) behavior was observed. 

*Keywords:* Catalytic packed bed; Nonlinear dynamics; Oscillations; Stability analysis; Numerical simulation

## 1. Introduction

Mechanisms for stationary pattern formation in chemically reacting systems have attracted significant attention since the pioneering work of Turing. The diffusive Turing instability (Turing, 1952) occurs in a two-variable system, when the inhibitor diffuses sufficiently faster than the activator (the autocatalytic variable). This mechanism was able to account for certain patterns in chemistry and biology, but largely was unable to induce patterns in liquid-phase liquid oscillatory reactions (like the Belousov–Zhabotinski), mainly since the reactants diffusivities are usually of similar magnitudes. It was also unable to account for catalytic patterns, in which the activator is typically long-ranged.

Recent works have pointed out that patterns may be induced by the interaction of kinetics and convection and this may have significant bearings on open chemical and catalytic reactors. These mechanisms require continuous supply of the reactants, either in the form of a cross-flow reactor or as a preceding reaction that occurs at a constant rate. While certain confusion still exists in interpreting these mechanisms we mention certain key references: In the DIFICI mechanism (Yakhnin, Rovinsky & Menzinger, 1994a,b, 1995) patterns emerge when the magnitude of the differential bulk flow exceed a critical value. Moving patterns due to the interaction of thermal bistability and feed dispersion along the reactor were suggested by us (Schvartsman & Sheintuch, 1995). Stationary space-periodic structures in a Brusselator were studied by Kuznetsov, Mosekilde, Dewel and Borckmans (1997), and Andresén, Bache, Mosekilde, Dewel and Borckmanns (1999), who also consider the interaction of this and a Hopf bifurcations. Finally, the authors (Nekhamkina, Nepomnyaschy, Rubinstein & Sheintuch, 2000a; Nekhamkina, Rubinstein & Sheintuch, 2000b) have recently studied the thermokinetic model of a catalytic reactor, with Danckwert's boundary conditions and realistic high *Le* and *Pe* values, showing a rich plethora of spatiotemporal patterns, including standing or moving waves and aperiodic patterns, that may emerge in such a system. We found that the moving waves that emerge in the convectively unstable unbounded system are usually arrested at the boundaries and above some amplification threshold stationary waves are established. Oscillatory or even chaotic behavior may emerge due to the

* Corresponding author. Tel.: + 972-4-8292823; fax: + 972-4-8230476.

*E-mail address:* cermsll@tx.technion.ac.il (M. Sheintuch).

0009-2509/01/$ - see front matter 
PII: S0009-2509(00)00288-8

interaction of the front-motion upstream and flow downstream. The thermokinetic model studied by us incorporated only concentration and temperature as its variables. In the present work we extended this analysis to account for reversible changes of the catalytic activity, as in a typical oscillatory catalytic system, and inquire whether that creates new types of behavior. We also draw the analogy between the distributed system and the simple CSTR problem with a modified Damkohler number.

In spatially extended systems with convection, like fixed-bed reactors, instabilities are referred to as either "convective" or as "absolute" when disturbances spread at velocities that are smaller or larger then the fluid velocity, respectively. In convectively unstable but absolutely stable bounded systems the amplified perturbations are ultimately swept out of the system leaving the reactor in its stationary state. Thus, perturbations cannot be sustained. A convectively unstable system may be made absolutely unstable by introducing a spatial feedback loop, for example, if the outlet stream is partially recycled. Such a mechanism was intensively employed in investigations of the DIFICI phenomena. Thus the boundary conditions are of considerable importance for the stability of the system. In real systems the inlet boundary conditions (for example, the Danckwert's type) are the sources of permanent perturbations. These perturbations in a convectively unstable region are amplified above some threshold value which in the general case does not correspond to the absolutely stability threshold (see the discussion in Nekhamkina et al., 2000a).

The advantages of the cross-flow reactor for certain classes of problems are listed in reaction engineering textbook: Gradual feeding of oxygen may improve selectivity in partial-oxidation reactions (Téllez, Menéndez & Santamaría, 1999) where high feed concentration leads to poor selectivity while low concentration limits the rate and conversion. By dispersing the feed along the reactor, in reactions with self-inhibition (typically described by Langmuir–Hinshelwood kinetics), we may maintain the reactant concentration at its optimal concentration, a value that leads to a maximal rate (Westerterp, Van Swaaij & Beenackers, 1984). The mass-supply and heat removal, required in such a system, is a challenging technical problem as it requires two interfaces within the reactor. We consider an annular tube with mass-transfer at one wall and heat-transfer at the other as a model of the system, while a multitube reactor incorporating two kinds of tubes for the two transfer processes is probably more practical. Radial gradients are expected in either case but we will ignore them here and describe the problem as one-dimensional. The unique aspect of such a reactor is that sufficiently far from the inlet the system approaches a homogeneous (space-independent) solution, which should be derived from certain optimization considerations.

The structure of this work is the following: in the next section the mathematical model is formulated, linear analysis is conducted in Section 3, in Section 4 the results of numerical simulations are presented and the comparison with analytical predictions is discussed, and in Section 5 the nonlinear analysis is conducted. In concluding remarks we briefly observe the main features that should be taken into account in the following studies.

## 2. Mathematical model

Consider the homogeneous one-dimensional model of a catalytic cross-flow reactor. Interphase gradients of temperature and concentration between the fluid and solid phases are assumed to be negligible. The mass and energy balances account for accumulation, convection, axial dispersion, chemical reaction $r(C,T,\varphi)$, heat loss due to cooling ($S_T = h_T P(T - T_w)$) and mass supply through a membrane wall ($S_C = k_g P(C - C_w)$):

$$\frac{\partial C}{\partial t} + u\frac{\partial C}{\partial z} - \varepsilon D_f \frac{\partial^2 C}{\partial z^2} = -(1-\varepsilon)r(C,T,\varphi) + S_C,$$

$$(\rho c_p)_e \frac{\partial T}{\partial t} + (\rho c_p)_f u\frac{\partial T}{\partial z} - k_e \frac{\partial^2 T}{\partial z^2} = (-\Delta H)(1-\varepsilon)r(C,T,\varphi) + S_T. \quad (1)$$

The Danckwert's boundary conditions are imposed at the inlet, while the no-flux condition — at the reactor exit

$$z = 0, \quad \varepsilon D_f \frac{\partial C}{\partial z} = u(C - C_{\text{in}}),$$

$$k_e \frac{\partial T}{\partial z} = (\rho c_p)_f u(T - T_{\text{in}}), \quad (2)$$

$$z = L, \quad \frac{\partial T}{\partial z} = \frac{\partial C}{\partial z} = 0.$$

We assume that the dispersion of mass is negligible. For a first-order activated kinetics, $r = A\varphi \exp(-E/RT)C$, where $\varphi$ is the dimensionless reversible catalytic activity, the system (1),(2) may be rewritten in the dimensionless form as

$$\frac{\partial x}{\partial \tau} + \frac{\partial x}{\partial \xi} = Da\,\varphi(1-x)\exp\left(\frac{\gamma y}{\gamma + y}\right) - \alpha_C(x - x_w) = f(x,y,\varphi),$$

$$Le\frac{\partial y}{\partial \tau} + \frac{\partial y}{\partial \xi} - \frac{1}{Pe}\frac{\partial^2 y}{\partial \xi^2} = B\,Da\,\varphi(1-x)\exp\left(\frac{\gamma y}{\gamma + y}\right) - \alpha_T(y - y_w) = g(x,y,\varphi), \quad (3)$$

$$\xi = 0, \quad x = 0, \frac{1}{Pe}\frac{\partial y}{\partial \xi} = y, \quad \xi = \tilde{L}, \frac{\partial y}{\partial \xi} = 0. \quad (4)$$

Here the conventional notation is used:

$$x = 1 - \frac{C}{C_{\text{in}}}, \quad y = \gamma \frac{T - T_{\text{in}}}{T_{\text{in}}}, \quad \xi = \frac{z}{z_0}, \quad \tau = \frac{tu}{z_0},$$
$$\gamma = \frac{E}{RT_{\text{in}}}, \quad B = \gamma \frac{(-\Delta H)C_{\text{in}}}{(\rho c_p)_f T_{\text{in}}},$$
$$Da = \frac{Az_0}{u} e^{-\gamma}, \quad Le = \frac{(\rho c_p)_e}{(\rho c_p)_f}, \quad Pe = \frac{(\rho c_p)_f z_0 u}{k_e}, \tag{5}$$
$$\alpha_C = \frac{k_g P z_0}{u}, \quad \alpha_T = \frac{h_T P z_0}{(\rho c_p)_f u}.$$

Note, that we did not use the reactor length $L$ as the length scale, but rather an arbitrary value $z_0$, so that $\tilde{L} = L/z_0$ can be varied as a free parameter. Typically the bed heat capacity is large ($Le \gg 1$) and $Pe \gg 1$. Note also that the conventional definition of Peclet is $Pe' = [(\rho c_p)_f Lu)]/k_e = Pe\,\tilde{L}$, so that in most simulations below $Pe' > 100$.

Our previous works assumed a constant activity ($\varphi \equiv 1$). Here we study the effect of varying $\varphi$. While there is no general agreement on the source of activation or deactivation, and their rates, we adopt here a simple linear expression (see Barto & Sheintuch, 1994; Sheintuch & Nekhamkina, 1999), that assumes that deactivation occurs faster at higher temperatures and at higher activities and that it is independent of reactant concentration, so that it can be expressed by a single line in the $(y,\varphi)$ phase plane. So the dimensionless form of the catalytic activity variation is

$$K_\varphi \frac{\partial \varphi}{\partial \tau} = a_\varphi - b_\varphi \varphi - y = h(y,\varphi) \tag{6}$$

and typically $K_\varphi \gg 1$. Recall that the time scale of autocatalytic thermal changes is $Le$, and changes of activity will be significant for $K_\varphi$ of similar magnitude as $Le$ or larger.

## 3. Stability analysis

In the limit of large Peclet numbers $Pe \to \infty$ the steady-state solutions of (3), (6), if they exist, are fully equivalent to the temporal solution of the following ODE system (with $\xi$ instead of $\tau$):

$$\frac{\partial x}{\partial \tau} = f(x,y,\varphi), \quad \frac{\partial y}{\partial \tau} = g(x,y,\varphi), \quad \varphi = \frac{a_\varphi - y}{b_\varphi}. \tag{7}$$

Thus the source of instability and many of its features can be studied from the related system (7). The dynamic behavior of the two equation system

$$\frac{\partial x}{\partial \tau} = f(x,y,1), \quad \frac{\partial y}{\partial \tau} = g(x,y,1), \tag{8}$$

has been extensively analyzed as it describes the temporal dynamics of a fluid-phase CSTR (e.g. Uppal, Ray & Poore, 1974, 1976; Guckenheimer, 1986). This problem can exhibit a plethora of phase plane regimes, including a simple limit cycle, a pair of stable and unstable limit cycles around a stable state, and so on.

As stated earlier system (3), (6) can attain a homogeneous steady-state in an unbounded system. The stability analysis of the full system was conducted in a standard manner (in an *unbounded system*). Denoting the deviation from the basic steady-state solution $\mathbf{u}_s = \{x_s, y_s, \varphi_s\}$ as $\mathbf{u}_1 = \{x_1, y_1, \varphi_1\}$, and linearizing the original problem, we arrive at the following system for the perturbations:

$$\frac{\partial \mathbf{u}_1}{\partial \tau} - \mathbf{V}\frac{\partial \mathbf{u}_1}{\partial \xi} - \mathbf{D}\frac{\partial^2 \mathbf{u}_1}{\partial \xi^2} = \mathbf{J}\mathbf{u}_1, \tag{9}$$

where $\mathbf{D} = \text{diag}\{0,\ (Le\,Pe)^{-1},\ 0\}$, and $\mathbf{V} = -\text{diag}\{1,\ Le^{-1}, 0\}$ are the diffusion and convection matrices. The matrix $\mathbf{J}$ can be found as a Jacobian matrix $\mathbf{F}_u, \mathbf{F}(\mathbf{u}) = \{f(\mathbf{u}), g(\mathbf{u})/Le, h(\mathbf{u})/K_\varphi\}$, calculated at the stationary point $\mathbf{u}_s$

$$\mathbf{J} = \begin{pmatrix} -\alpha_C - G(y_s)Z(y_s) & G'(y_s)Z(y_s)H(y_s)/B & H(y_s)/BG(y_s) \\ -BG(y_s)Z(y_s)/Le & (Z(y_s)G'(y_s)H(y_s) - \alpha_T)/Le & H(y_s)/Le\,G(y_s) \\ 0 & -1/K_\varphi & -b_\varphi/K_\varphi \end{pmatrix},$$

where $H(y) = B(1 - x_w) - (\alpha_T/\alpha_C)(y - y_w)$, $G(y) = Da \exp((\gamma y)/(\gamma + y))$, $Z(y) = (a_\varphi - y)/b_\varphi$.

Assuming the perturbations to be harmonic in the space variable $\xi$, i.e., $\mathbf{u}_1 = \{x_1, y_1, \varphi_1\} = a\mathbf{U}e^{ik\xi + \sigma\tau}$, where $k$ is the perturbation wave number, $\sigma$ is the time growth rate, $\mathbf{U}$ an eigenvector, and using it in (9), we obtain the dispersion relation $\mathscr{D}(\sigma, k) = 0$. It has a form of the cubic equation with *complex* coefficients:

$$\sigma^3 + A\sigma^2 + P\sigma + Q = 0. \tag{10}$$

The free term is $Q = \det \mathbf{M}$, where

$$\mathbf{M} = \mathbf{J} + ik\mathbf{V} - k^2\mathbf{D}. \tag{11}$$

The neutral curve defined by the bifurcation condition $Re\,\sigma = 0$ may be calculated numerically for a specified set of parameters. We used $Pe$ as the bifurcation parameter as it does not influence the steady-states solutions. (Moreover, as it was mentioned above, the stationary patterns emerging at $Pe \to \infty$ for system (3), (6) correspond to the dynamic behavior of the related CSTR problem; this observation will be useful for analysis of the

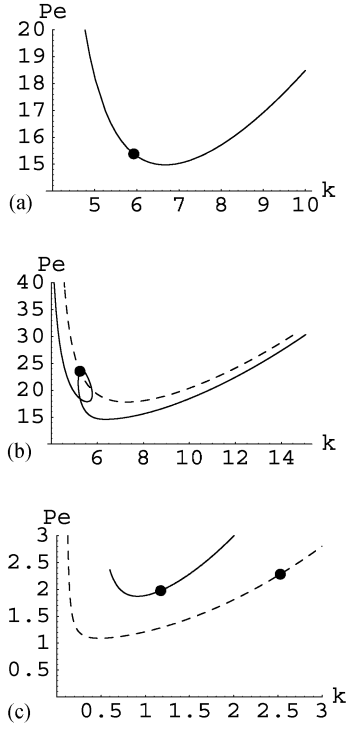


Fig. 1. Neutral curves: (a): $B = 16.2$, $\alpha = 4, Da = 0.2$, $\varphi \equiv 1$ (as in fig. 17, Uppal et al., 1974), (b): varying $\varphi$ case with $a_\varphi = B, K_\varphi = 10^4$ (solid line) or $K_\varphi = 10^2$ (dash line; other parameters as in (a); (c): $B = 16.2$, $\alpha = 4, Da = 0.132$, $\varphi \equiv 1$ (as in fig. 18, Uppal et al., 1974). The solid and dash lines in (c) correspond to the lower and upper steady-state solutions. The dot denotes the amplification threshold $(Pe_0, k_0)$.

system behavior, as we show below.) The neutral curve typically acquires a minimum $k_c, Pe_c$ (see Fig. 1) and crossing $Pe_c$ corresponds to an excitation of oscillatory solutions with finite $k$ in an *unbounded* system, or in a ring-shaped system, moving at a constant speed.

The behavior of a *bounded* system is markedly different due to the Danckwert's boundary conditions. Below a certain "amplification" threshold $Pe = Pe_0$ the perturbations are ultimately swept out of the system leaving the reactor in its stationary state. This threshold was found to be a point at the neutral curve where the frequency of the emerging oscillatory patterns $\omega$ is equal to zero, i.e. Im $\sigma = 0$. We found that the system typically admits a solution close to the homogeneous one for $Pe < Pe_0$. Stationary patterns typically emerge above the critical point $Pe > Pe_0$. Note that the wavelength $2\pi/k$ in a sufficiently long system is independent of the boundary conditions and is determined solely by kinetic parameters. That applies for $k_c$ or $k_0$ and as we see below for transients that include both wave numbers.

The critical parameters may be determined analytically:

$$k_0 = (Z(y_s)G(y_s)H(y_s)(Z(y_s)G'(y_s) + Z(y_s)'G(y_s)) - (\alpha_C + Z(y_s)G(y_s))^2)^{1/2},$$

$$Pe_0 = -\frac{k_0^2}{\alpha_C + \alpha_T + Z(y_s)G(y_s) - H(y_s)(Z(y_s)G'(y_s) + Z(y_s)'G(y_s))}. \quad (12)$$

For the constant activity case a plot of $y_s = y_s(Da)$ and the corresponding $Pe_0$ and $k_0$ for a set of parameters for which a region of multiplicity exists (Fig. 2a–c) show multiple critical points corresponding to the appropriate steady states. The lines in Fig. 2b extend to $Pe_0 \to \infty$ which implies that the denominator of Eq. (12) vanishes. That is simply the condition for appearance of oscillations in the corresponding CSTR model. This condition is useful in determining the range of parameters $(Da)$ where the instability appears.

For the variable $\varphi$ model we used $a_\varphi$ as a free parameter and define $b_\varphi = a_\varphi - y_s$ in order to ensure the same set of the steady-state solution of the full system $y_s, x_s$ with $\varphi_s = 1$. Typical dependences of $Pe_0, k_0$ on $a_\varphi$ are plotted in Fig. 2d and e. Obviously $\varphi_s \to 1$ with $a_\varphi \to \infty$ and the critical parameters tend to the asymptotic values corresponding to the two variable systems with regular kinetics.

## 4. Numerical simulations

In this section we analyze the spatiotemporal patterns that emerge in the distributed system (3), (4) with fixed or variable catalytic activity for some typical cases that were investigated for the related CSTR problem by Uppal et al. (1974). To be consistent with that study we set without loss of generality $x_w = y_w = 0$, (i.e. supply conditions are similar to feed conditions), $\alpha_c = 1$, and $\alpha_T = \beta + 1$ ($\beta$ is a coefficient used in Uppal et al. (1974) to describe heat transfer). In all simulations we choose $Le = 100$ and the reactor length was set $\tilde{L} = 10$–$25$ in order to resolve a structure of the emerging patterns.

*Case* 1: The simplest CSTR dynamics (aside for a stable state) is one that admits an unstable steady-state solution $(y_s, x_s)$ surrounded by a stable limit cycle. The corresponding neutral curve for $\varphi \equiv 1$ case typically acquires the form of Fig. 1a and includes a critical point $(Pe_0, k_0)$. The form of the curve for the variable $\varphi$ system drastically depends on the parameters of the third equation. For $a_\varphi \gg y_s$ and $K_\varphi \sim Le$ the neutral curve (Fig. 1b, dash line) is shifted but preserves the same form as for the constant activity case. With increasing $K_\varphi$ the neutral curve changes significantly (compare the solid and dash lines in Fig. 1b), but the critical values $Pe_0, k_0$ corresponding to the emergence of the stationary patterns obviously do not depend on the time scales.

Consider the system behavior for a set of parameters that corresponds to relatively small oscillations of the catalytic activity (as in Fig. 1b, $K_\varphi = Le = 100, a_\varphi = y_s$)

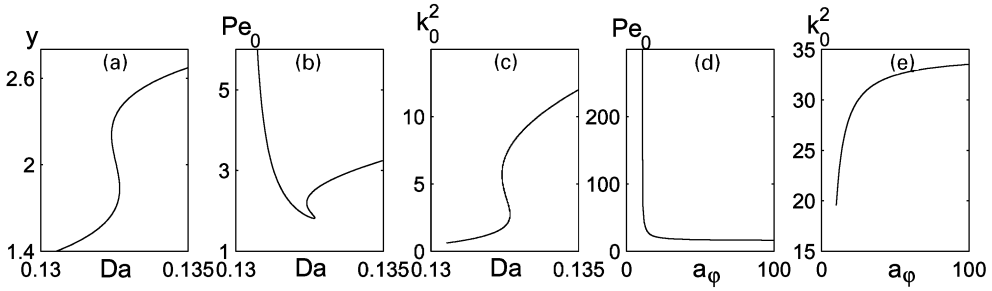


Fig. 2. Steady states $y_s$ (a), critical $Pe_0$ (b) and $k_0$ (c) in a region of multiplicity for the constant activity case: $B = 16.2$, $\alpha = 4$, $\varphi \equiv 1$ (as in fig. 16 Uppal et al., 1974), $Le = 100$; dependence of $Pe_0$ (d) and $k_0$ (e) on the activity variation parameter $a_\varphi$ $K_\varphi = 100, b_\varphi = a_\varphi - y_s, B = 16.2$, $\beta = 3, Da = 0.2$.

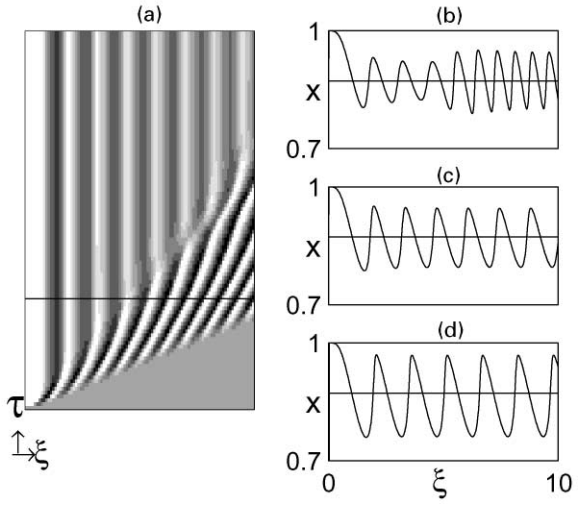


Fig. 3. (a) The transient leading to formation of the stationary patterns ($Pe = 30$); temperature is denoted as a gray scale in the time vs. space plane; (b) The transient profile of the dimensionless concentration ($x$) for $Pe = 30$ (the corresponding moment is marked by a line in (a)); (c and d): Steady-state profiles of ($x$) for $Pe = 50$ and 1000. The horizontal lines in (b–d) show the steady-state level. (Small variations of the catalytic activity, $a_\varphi = 2y_s$, $\tilde{L} = 10$, other parameters as in fig. 1a.

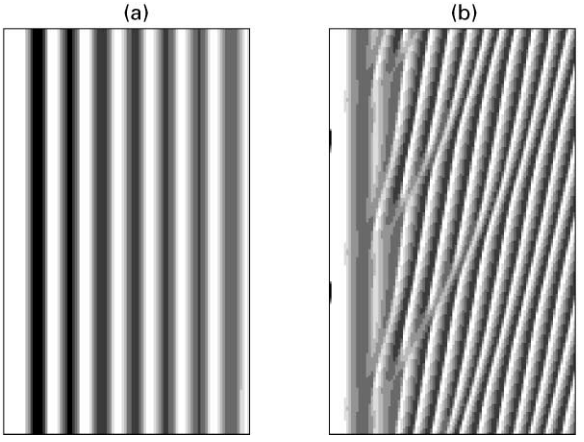


Fig. 4. Effect of the time scale on the pattern selection for the oscillatory kinetics model: stationary waves with $K_\varphi = 10^2$ (a), aperiodic moving waves with $K_\varphi = 10^4$ (b). $a_\varphi = 1.5y_s$, other parameters as in Fig. 1b.

and varying $Pe$. Stationary patterns were obtained for all $Pe$ values. For $Pe < Pe_c$ the homogeneous solution is established in most of the domain with some adjustment at the inlet section, due to the boundary conditions. For $Pe_c < Pe < Pe_0$ the system exhibits transients of traveling waves that are washed out of the reactor. In the supercritical region $Pe > Pe_0$ the moving waves are consequently arrested and rearranged in a system of spatially periodic standing waves. The typical dynamic behavior is presented in Fig. 3a, and the profile transformation is illustrated by Fig. 3b–d. Two different regimes are clearly distinguished in Fig. 3b: $\xi > 5$ corresponds to traveling waves of constant amplitude with $k \simeq k_c$, while near the inlet we observe the standing waves with $k \simeq k_0 < k_c$ and a variable amplitude that tends to some saturated value which is less than the amplitude of the moving waves. For relatively small deviations from the bifurcation the stationary patterns have an harmonic form and the computed wave number is in very good agreement with the theoretical value $k_0$ (Eq. (12)). With increasing $\Delta Pe \equiv Pe - Pe_0$ the amplitude of the state variables grows, the patterns become highly nonlinear (saw-tooth pattern) and the wave number decreases (see Fig. 3d). Numerical simulations reveal that the structure of the patterns become insensitive to $Pe$ number for large $Pe$ ($> 10^3$) and, as expected, the form of the stationary spatial patterns completely corresponds to the dynamic behavior of the related modified CSTR model.

With decreasing $a_\varphi$ ($a_\varphi \to y_s$) the mechanism of patterns selection changes drastically. In the supercritical region the system exhibits moving aperiodic waves which may be "arrested" by the boundaries only for relatively small deviations $\Delta Pe = Pe - Pe_0$. The range of $Pe$, for which the stationary patterns are established decreases with increasing $K_\varphi$ (see Fig. 4). For $Pe \gg Pe_0$ a chaotic behavior was observed in many cases but its classification is rather cumbersome and will be considered in the following work.

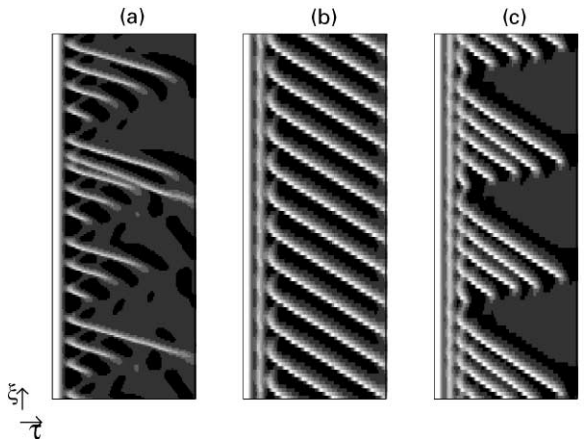


Fig. 5. Effect of $Pe$ on the spatiotemporal patterns for case 2, $\varphi \equiv 1$ ($\tilde{L} = 25$): 2.1 (a — aperiodic behavior), 3.0 (b — period-1 patterns), 3.5 (c — period-5 packet), other parameters as in Fig. 1c.

*Case* 2. This case corresponds to a CSTR problem which admits three unstable steady states surrounded by a single stable limit cycle (The set of parameters corresponds to Fig. 1c.). The simulations were carried out for a fixed activity case ($\varphi \equiv 1$), and even for this system the chaotic behavior was observed as will be shown below.

The neutral curves calculated for the lower $(x_{s1}, y_{s1})$ and upper $(x_{s3}, y_{s3})$ steady-state solutions exhibit local minima and critical amplification points (Fig. 1c). For $Pe < \min(Pe_{c1}, Pe_{c3})$ only stationary solutions, depending on the initial conditions are obtained. (In the following calculations we used the intermediate steady state $(x_{s2}, y_{s2})$ as the initial conditions.) In a domain which roughly lies around the two critical $Pe$ the system exhibits spatiotemporal patterns in which a pulse is born somewhere downstream and then moves upstream and disappears. The motion is periodic if the birthpoint of this pulse is reproduced on successive pulses, or multiperiodic or even aperiodic when it does not repeat itself. Aperiodic behavior is recorded for $Pe = 2.1$–$2.3$ (Fig. 5a). Regular period-5 patterns are established at $Pe = 2.5$. The short waves are consequently followed by the longer waves forming a single packet. At $Pe = 3.0$ regular moving patterns that span most of the reactor are established (Fig. 5b). Period-5 patterns are maintained again in the range $3 < Pe < 4$ but unlike the lower $Pe$ regimes, a single standing wave is already formed near the inlet (compare Fig. 5a and c).

The stationary patterns are established for $Pe > 5$. This value differs sufficiently from the critical amplification numbers, calculated for both lower and upper steady-state solutions, and the computed wave number also does not agree with any of the analytical values. With increasing $Pe$, the standing wave patterns fully correspond to the temporal solution of the related CSTR problem.

## 5. Nonlinear analysis

While we do not present here the nonlinear analysis of system (3), (6), we recall recent results of the constant activity ($\varphi \equiv 1$) case (Nekhamkina et al., 2000a). Nonlinear analysis may provide some general results of the system behavior, but its application is limited to an unbounded system or a system with periodic boundary conditions. We introduced a hierarchy of time and spatial scales

$$\partial/\partial t = \partial/\partial t_0 + \varepsilon\partial/\partial t_1 + \varepsilon^2\partial/\partial t_2 + \cdots,$$

$$\partial/\partial \xi = \partial/\partial \xi_0 + \varepsilon^\beta\partial/\partial \xi_1 + \cdots, \tag{13}$$

here the value of $\beta$ should be chosen to balance properly terms of different orders of $\varepsilon$. The critical point $(k_0, Pe_0)$ is usually located at the linear section of the neutral curve, so it is reasonable to set $\beta = 2$.

We also expand in Taylor series the phase variables and the bifurcation parameter

$$\mathbf{u} = \mathbf{u}_0 + \varepsilon\mathbf{u}_1 + \varepsilon^2\mathbf{u}_2 + \cdots,$$

$$Pe = Pe_0 + \varepsilon Pe_1 + \varepsilon^2 Pe_2 + \cdots. \tag{14}$$

Substituting the above expansions into the original set of equations, and collecting terms of the same orders of $\varepsilon$ we produce a set of equations. The resulting amplitude equation has the following form:

$$\frac{\partial a}{\partial t_2} = -c_3|a|^2 a + c_1 a + v\frac{\partial a}{\partial \xi_1}. \tag{15}$$

It should be emphasized that Eq. (15) is actually ill-posed, i.e, infinitesimally small perturbations of a solution will grow very fast, so that the original approximation is no longer justified. However this equation is useful for analysis of two different cases: (i) when the spatial modulation of the amplitude is neglected ($\partial a/\partial \xi_1 = 0$) thus the wave number is prescribed; or (ii) for the calculation of the spatially modulated *steady-state* regime ($\partial a/\partial t_2 = 0$) where the short-wave modulations which grow fast are excluded from consideration.

The comparison of the nonlinear stability analysis results with numerical simulations is a rather cumbersome problem. The simplest way to check the regime with constant amplitudes is to simulate the reactor with periodic boundary conditions (corresponds to case (i) mentioned above). As was demonstrated for the constant activity case $\varphi \equiv 1$ (Nekhamkina et al. 2000a), in the degenerate case when the critical points $Pe_0, k_0$ and $Pe_c, k_c$ coincide, the analytical and numerical amplitudes and velocities are in a very good agreement for small deviations in $\Delta Pe$.

The Danckwert's boundary conditions produce in the general case very high perturbations, which cannot be

taken into account by the weak stability analysis. The saturated amplitudes, obtained in numerical simulation preserve the linear dependence on $\sqrt{\Delta Pe}$ for small $\Delta Pe/Pe$(5–10%) but the slope of these lines differs from the analytical values (by 20–40%).

## 6. Concluding remarks

This work extends our analysis of the mechanism of patterns formation in the relatively simple model of a homogeneous model of a cross-flow catalytic reactor. Patterns emerge due to convection–reaction interaction and are different than the classical Turing patterns. They are different also from recent mechanisms of pattern formation in open flow systems as the constant-activity system here cannot exhibit a Hopf bifurcation due to the large heat capacity ($Le \gg 1$). Both linear and weakly nonlinear stability analysis were carried out using $Pe$ number as a bifurcation parameter. For the limit case $Pe \to \infty$ we draw the analogy between the stationary patterns in the distributed system (where $Le \gg 1$) with the temporal behavior of the corresponding gas-phase CSTR problem (i.e., $Le = 1$). For finite $Pe$ values in the vicinity of the bifurcation point the spatiotemporal behavior drastically depends on the type of a phase plane. Only stationary patterns emerge in the distributed system for the simplest dynamics which in a CSTR admits an unstable steady-state solution surrounded by a stable limit cycle. For more complicated cases, especially for the cases when the corresponding CSTR problem admits multiple unstable steady states, both regular and aperiodic behaviors were observed which obviously cannot be predicted by the stability analysis.

The emerging patterns are of great academic interest, but we would like to discuss here the feasibility of their experimental realizations. As we noted above the phenomena will appear in thermokinetic systems that admit oscillatory behavior in their $Le = 1$ version, which applies to many oxidation, hydrogenation and other reactions. The minimal reactor length to observe this behavior is the wavelength, which for practical problems is an acceptable length. While we employed a "generic" model to show the emergence of nonTuring stationary patterns, more realistic models will use other features as well which will be considered in future works. One feature we want to consider is the effect of a coreactant, as in an oxidation reaction, where the first (say the fuel, $C_B$) is supplied with the flow so its rate follows $k(T)f(C_B)C_A$, where $f(C_B)$ is taken to be of the form $C_B/(1 + KC_B)$, while the second (say oxygen, $C_A$) is supplied continuously at high concentration. In the limit of very large $K$ the problem reduces to the previous one ($\varphi \equiv 1$), except when $C_B$ is exhausted and the term $KC_B$ becomes small. In a second modification we want to consider the effect of a second reaction (i.e., two consecutive reactions, partial and complete oxidation) that kicks off at higher temperatures (high activation energies). The design should avoid the occurrence of a second reaction so that the temperature should not exceed the complete oxidation reaction. Another feature is the existence of heat and mass transfer gradients between the phases; the results of this "heterogeneous model" may be significantly different than those of the homogeneous model described above. Specifically, the interphase gradients will diminish the effect of inlet boundary conditions and give rise to moving patterns rather than stationary ones. This possibility was pointed out in a learning model using "polynomial" kinetics (Schvartsman & Sheintuch, 1995), that was tailored to mimic a heterogeneous reactor model.

The present work as well as the previous studies may be considered as first steps in the simulation and operation of a growing class of reactors with a complex spatiotemporal dynamics; these include the reverse-flow reactor, and the circulating loop reactor.

## Notation

| | |
|---|---|
| $B$ | dimensionless exothermicity |
| $c_p$ | volume-specific heat capacity |
| $C$ | key component concentration |
| $D$ | axial dispersion coefficient |
| $E$ | activation energy |
| $\Delta H$ | reaction enthalpy |
| $Da$ | Damkohler number |
| $k$ | thermal conductivity |
| $L$ | reactor length |
| $Le$ | Lewis number |
| $Pe$ | Peclet number |
| $r$ | reaction rate |
| $u$ | fluid velocity |
| $t$ | time |
| $T$ | temperature |

*Greek letters*

| | |
|---|---|
| $\alpha_T$,$\alpha_C$ | heat and mass transfer coefficients |
| $\varepsilon$ | bed void fraction |
| $\rho$ | density |
| $\varphi$ | dimensionless catalytic activity |

*Subscripts*

| | |
|---|---|
| $e$ | effective value |
| $f$ | fluid |
| in | at the inlet |
| $s$ | solid |
| $w$ | wall value |
| $\varphi$ | activity parameter |

## Acknowledgement

This work was supported by the Volkswagen-Stiftung Foundation. M.S. and B.R. are members of the Minerva Center of Nonlinear Dynamics. O.N. is partially supported by the Center for Absorption in Science, Ministry of Immigrant Absorption State of Israel.

## References

Andresén, P., Bache, M., Mosekilde, E., Dewel, G., & Borckmanns, P. (1999). Stationary space-periodic structures with equal diffusion coefficients. *Physics Review E*, *60*, 297.

Barto, M., & Sheintuch, M. (1994). Excitable waves and spatiotemporal patterns in a fixed-bed reactor. *A.I.Ch.E Journal*, *40*, 120.

Guckenheimer, J. (1986). Multiple bifurcation problems for chemical reactors. *Physica*, *20D*, 1.

Kuznetsov, S. P., Mosekilde, E., Dewel, G., & Borckmans, P. (1997). Absolute and convective instabilities in a one-dimensional Brusselator flow model. *Journal of Chemical Physics*, *106*, 7609–7616.

Nekhamkina, O., Nepomnyaschy, A., Rubinstein, B., & Sheintuch, M. (2000a). Nonlinear analysis of stationary patterns in convection–reaction–diffusion systems. *PRE*, *61*, 2436–2444.

Nekhamkina, O., Rubinstein, B., & Sheintuch, M. (2000b). Spatiotemporal patterns in thermokinetic models of cross-flow reactors. *A.I.Ch.E. Journal*, *46*, 1632–1640.

Schvartsman, S., & Sheintuch, M. (1995). One- and two-dimensional spatiotemporal patterns in a fixed-bed reactor. *Chemical Engineering Science*, *50*, 3125.

Sheintuch, M., & Nekhamkina, O. (1999). Pattern formation in homogeneous reactor models. *A.I.Ch.E Journal*, *45*, 398.

Turing, A. M. (1952). The chemical basis for morphogenesis. *Philosophical Transactions of the Royal Society B*, *237*, 37–72.

Téllez, C., Menéndez, M., & Santamaría, J. (1999). Simulation of an inert membrane reactor for the oxidative dehydrogeneration of butane. *Chemical Engineering Science*, *54*, 2917.

Uppal, A., Ray, W. H., & Poore, A. B. (1974). On the dynamic behavior of continuous stirred tank reactors. *Chemical Engineering Science*, *29*, 967.

Uppal, A., Ray, W. H., & Poore, A. B. (1976). The classification of the dynamic behavior of continuous stirred tank reactors-influence of reactor residence time. *Chemical Engineering Science*, *31*, 205.

Westerterp, K. R., Van Swaaij, W. P. M., & Beenackers, A. A. C. M. (1984). *Chemical reactor design and operation*. New York: Wiley.

Yakhnin, V. Z., Rovinsky, A. B., & Menzinger, M. (1994a). Differential flow instability of the exothermic standard reaction in a tubular cross-flow reactor. *Chemical Engineering Science*, *49*, 3257.

Yakhnin, V. Z., Rovinsky, A. B., & Menzinger, M. (1994b). Differential-flow-induced pattern formation in the exothermic $A \rightarrow B$ reaction. *Journal of Physics Chemistry*, *98*, 2116.

Yakhnin, V. Z., Rovinsky, A. B., & Menzinger, M. (1995). Convective instability induced by differential transport in the tubular packed-bed reactor. *Chemical Engineering Science*, *50*, 2853.